Constrained periodic spacecraft relative motion using non-negative polynomials

Georgia Deaconu, Christophe Louembet, Alain Théron

Constrained periodic spacecraft relative motion using non-negative polynomials

G. Deaconu, C. Louembet and A.Théron
CNRS ; LAAS ; 7 Avenue du colonel Roche, F-31077 Toulouse; France
Université de Toulouse; UPS, INSA, ISAE; UT1, UTM, LAAS; F-31077 Toulouse; France

***Abstract*— A new method for obtaining constrained periodic relative motion between spacecraft on Keplerian orbits is presented. The periodic relative trajectory is required to evolve autonomously inside a tolerance box centered in a specified position. Unlike the classical time-sampling approaches, our method guarantees continuous satisfaction of the constraints on infinite horizon. This is done by reformulating the tolerance box constraints on the relative trajectory as conditions of non-negativity of some polynomials. The resulting problem is solved using semi-definite programming.**

***Keywords*— impulsive orbital rendezvous, periodic relative motion, non-negative polynomials, semi-definite programming,**

I. INTRODUCTION

In the recent years, new rendezvous missions and proximity operations between spacecraft have been considered, including sample returns, repairing, refueling, upgrading, and other on-orbit servicing [1]. The ability to design fuel efficient maneuvers in order to reach naturally periodic relative orbits, confined in a specified region in space, will be an important step towards the success of these missions. We propose a new method for obtaining an open loop maneuvers plan leading to this kind of bounded autonomous periodic motion.

The relative motion between spacecraft on Keplerian orbits is naturally bounded [2]. Moreover, the relative motion can be initialized to result as periodic when viewed from a local reference frame. In the unperturbed case, the necessary and sufficient condition for periodicity is that the semi-major axis of the spacecraft orbits are equal [3]. The period of the resulting relative trajectory is then equal to the orbital period of the spacecraft.

Using Cartesian coordinates and a local frame attached to one of the spacecraft, Inalhan obtained in [4] a periodicity condition at perigee, for the linearized relative motion and for arbitrary eccentricity. This condition was then used for spacecraft formation initialization. Inalhan's condition was later explicitly generalized for any true anomaly in [5], where the effect of the eccentricity on the shape of the periodic relative trajectory was analyzed. Gurfil wrote the energy-matching condition for periodicity in [2], obtaining a sixth degree polynomial equation, valid for the non linear dynamics.

The previous conditions guarantee that the resulting relative trajectory will be periodic, without giving any insight on its shape or its size. In [6] and [7], Gurfil and Kolshevnikov analytically studied the minimum and maximum distances between two spacecraft on elliptical orbits. Their method amounts to solving an eighth degree trigonometric polynomial and obtaining the true anomalies corresponding to the extremal distances, in a worst case analysis. However, the dimensions of the relative trajectory are highly dependent on the initial conditions of the motion, which are not considered in the aforementioned studies.

In [8] model predictive control (MPC) and linear programming (LP) are used to design a fuel optimal maneuvers plan, leading to autonomous periodic relative motion confined inside a specified tolerance region. The method is based on the propagation of the autonomous relative motion starting at the end of the plan for one additional orbital period. Periodicity is ensured by imposing the initial and the final state of the autonomous motion to match. To control the dimensions of the periodic trajectory, its inclusion in the tolerance box is explicitly checked in a finite number of time samples along the propagation. Because of the nature of the orbital dynamics, an autonomous relative trajectory that remains inside the box for one orbit and begins and terminates at the same state is a nominal invariant set [8]. Thus attaining this kind of trajectory prevents any future constraints violation.

The LP formulation has the advantage of providing a general framework for minimizing fuel consumption while including various types of state and actuator constraints [9]. The drawback is that it cannot guarantee continuous satisfaction of the constraints since the behavior between the time samples is not controlled.

A new method for designing a fuel optimal maneuvers plans leading to this type of bounded periodic relative motion is presented in this paper. This approach no longer requires the explicit propagation of the autonomous relative trajectory at specified time samples. It is based on the fact that the periodic motion can be represented by rational expressions. We show that, by using these rational expressions, the dimension constraints for the periodic trajectory can be written in terms of non-negativity of some polynomials. The main advantage of this method is that it guarantees constraints satisfaction *continuously in time*.

The paper is organized as follows. Section II first gives a brief description of the spacecraft relative dynamics and their closed-form solutions. Then the linear condition used to ensure the periodicity of the relative trajectory is presented.

Finally, the rational expressions for the propagation of the autonomous periodic relative motion are derived. Our main contribution is detailed in Section III, where the previously obtained rational expressions are used to write the problem of designing a periodic relative trajectory contained in a tolerance box as a polynomial optimization problem. This polynomial optimization problem is transformed into a convex semi-definite program (SDP), for which efficient solvers are available. An always feasible formulation of the problem is also presented, by considering the dimensions of the tolerance box as part of the optimization variables. The methodology is illustrated through some impulsive rendezvous scenarios in Section IV.

II. Relative Dynamics and Periodicity

A. Relative Motion Modeling

Let us consider the relative motion between two spacecraft on elliptic Keplerian orbits. The reference orbit corresponds to the leader spacecraft M_1 while the other orbit corresponds to the follower spacecraft M_2.

Consider an Earth-centered inertial (ECI) frame with the orthonormal basis $B_0 = (\vec{X}_0, \vec{Y}_0, \vec{Z}_0)$. The relative motion is described in the rotating Cartesian local-vertical/local-horizontal (LVLH) frame attached to the leader. The corresponding basis is $B_1 = (\vec{x}_1, \vec{y}_1, \vec{z}_1)$, with $\vec{z}_1$ lying along the radius vector from the satellite to the center of the Earth, $\vec{y}_1$ normal to the plane defined by the position and velocity vectors of M_1 in the ECI frame, in opposite direction to the angular momentum, and $\vec{x}_1$ completing the basis (Fig. 1).

Let $\vec{r} = \begin{bmatrix} x & y & z \end{bmatrix}^T$ be the position of the follower spacecraft in the LVLH frame of the leader. The linearized relative dynamics with respect to the orbit of the leader are described by the well-known Tschauner-Hempel equations [10]:

$$\begin{aligned} \ddot{x} &= 2\dot{\nu}\dot{z} + \ddot{\nu}z + \dot{\nu}^2 x - \frac{\mu}{R^3}x + u_x \\ \ddot{y} &= -\frac{\mu}{R^3}y + u_y \\ \ddot{z} &= -2\dot{\nu}\dot{x} - \ddot{\nu}x + \dot{\nu}^2 z + 2\frac{\mu}{R^3}z + u_z \end{aligned} \tag{1}$$

where ν and R are the true anomaly and the norm of the radius of the leader, μ is the gravitational parameter of the Earth:

$$\dot{\nu} = \sqrt{\frac{\mu}{a^3(1-e^2)^3}}(1+e\cos\nu)^2, \quad R = \frac{a(1-e^2)}{1+e\cos\nu}, \tag{2}$$

and a and e are the semi-major axis and the eccentricity of the leader. After replacing time as the independent variable with the true anomaly:

$$\frac{d(\cdot)}{dt} = \frac{d(\cdot)}{d\nu}\frac{d\nu}{dt} = (\cdot)'\dot{\nu}, \quad \frac{d^2(\cdot)}{dt^2} = \dot{\nu}^2(\cdot)'' + \ddot{\nu}(\cdot)' \tag{3}$$

and scaling the variables by:

$$\begin{aligned} \begin{bmatrix} \tilde{x} \\ \tilde{y} \\ \tilde{z} \end{bmatrix} &= (1+e\cos\nu)\begin{bmatrix} x \\ y \\ z \end{bmatrix} \\ \begin{bmatrix} \tilde{x}' \\ \tilde{y}' \\ \tilde{z}' \end{bmatrix} &= (1+e\cos\nu)\begin{bmatrix} x' \\ y' \\ z' \end{bmatrix} - e\sin\nu\begin{bmatrix} x \\ y \\ z \end{bmatrix} \end{aligned}, \tag{4}$$

equations (1) become:

$$\begin{aligned} \tilde{x}'' &= 2\tilde{z}' + \tilde{u}_x \\ \tilde{y}'' &= -\tilde{y} + \tilde{u}_y \\ \tilde{z}'' &= \tfrac{3}{1+e\cos\nu}\tilde{z} - 2\tilde{x}' + \tilde{u}_z \end{aligned} \tag{5}$$

In the sequel, the $\tilde{}$ sign is used to mark the variables after the variables change (4). If we define the state vector $\tilde{X}(\nu) = \begin{bmatrix} \tilde{x}(\nu) & \tilde{y}(\nu) & \tilde{z}(\nu) & \tilde{x}'(\nu) & \tilde{y}'(\nu) & \tilde{z}'(\nu) \end{bmatrix}^T$ and the input vector $\tilde{u}(\nu) = \begin{bmatrix} \tilde{u}_x(\nu) & \tilde{u}_y(\nu) & \tilde{u}_z(\nu) \end{bmatrix}^T$, system (5) can be written as a periodic state-space model:

$$\frac{d\tilde{X}(\nu)}{d\nu} = \tilde{A}(\nu)\tilde{X}(\nu) + \tilde{B}\tilde{u}(\nu) \tag{6}$$

with:

$$\tilde{A}(\nu) = \begin{bmatrix} 0 & 0 & 0 & 1 & 0 & 0 \\ 0 & 0 & 0 & 0 & 1 & 0 \\ 0 & 0 & 0 & 0 & 0 & 1 \\ 0 & 0 & 0 & 0 & 0 & 2 \\ 0 & -1 & 0 & 0 & 0 & 0 \\ 0 & 0 & \frac{3}{1+e\cos\nu} & -2 & 0 & 0 \end{bmatrix}, \quad \tilde{B} = \begin{bmatrix} 0 & 0 & 0 \\ 0 & 0 & 0 \\ 0 & 0 & 0 \\ 1 & 0 & 0 \\ 0 & 1 & 0 \\ 0 & 0 & 1 \end{bmatrix} \tag{7}$$

Starting from system (6), Yamanaka and Ankersen give in [11] a transition matrix Φ which enables the propagation of the relative motion starting from an initial condition $\tilde{X}(\nu_0)$, under impulsive control:

$$\tilde{X}(\nu) = \Phi_{\nu_0}^{\nu}\tilde{X}(\nu_0) + \sum_i \Phi_{\nu_i}^{\nu}\tilde{B}\tilde{u}_i. \tag{8}$$

B. Periodic motion propagation

An arbitrary state $\tilde{X}(\nu_0)$ is an initial state for a naturally periodic motion if it is equal to the autonomously propagated state after one period. This condition can easily be expressed using the Yamanaka-Ankersen transition matrix:

$$\tilde{X}(\nu_0 + 2\pi) = \Phi_{\nu_0}^{\nu_0+2\pi}\tilde{X}(\nu_0) = \tilde{X}(\nu_0) \tag{9}$$

After some calculations, the following periodicity condition is obtained [5]:

$$\tilde{x}'(\nu_0) = \frac{(2+3e\cos\nu_0+e^2)}{(1+e\cos\nu_0)^2}\tilde{z}(\nu_0) + \frac{e\sin\nu_0}{(1+e\cos\nu_0)}\tilde{z}'(\nu_0). \tag{10}$$

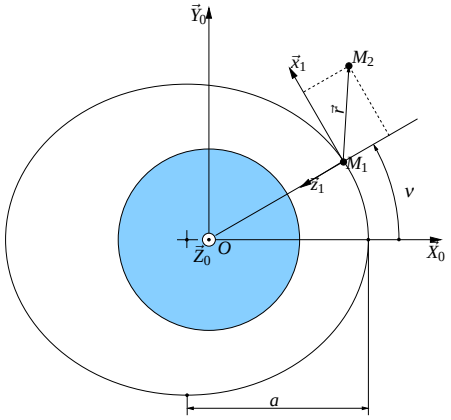

Fig. 1. The local frame and the relative position of the spacecraft

Considering $u_i = 0$ in (8) and assuming that the initial state $\tilde{X}(\nu_0)$ satisfies (10), the equations for the propagation of the periodic motion can be deduced:

$$\begin{array}{l} \tilde{x}(\nu) = (2+e\cos\nu)(d_1\sin\nu - d_2\cos\nu) + d_3 \\ \tilde{y}(\nu) = d_4\cos\nu + d_5\sin\nu \\ \tilde{z}(\nu) = (1+e\cos\nu)(d_1\cos\nu + d_2\sin\nu) \end{array} \quad , \ \nu \geq \nu_0 \tag{11}$$

where $d_i,\ i = 1...5$ are constants linearly depending on the initial state $\tilde{X}(\nu_0)$. Let $D = \begin{bmatrix} d_1 & d_2 & d_3 & d_4 & d_5 \end{bmatrix}^T$, then:

$$D = C(\nu_0)\tilde{X}(\nu_0) \tag{12}$$

where the matrix $C(\nu_0)$ is defined by:

$$C(\nu_0) = \begin{bmatrix} 0 & 0 & \frac{2ec_0^2+c_0-e}{(1+ec_0)^2} & 0 & 0 & -\frac{s_0}{1+ec_0} \\ 0 & 0 & \frac{s_0(1+2ec_0)}{(1+ec_0)^2} & 0 & 0 & \frac{c_0}{1+ec_0} \\ 1 & 0 & \frac{es_0(2+ec_0)}{(1+ec_0)^2} & 0 & 0 & \frac{2+ec_0}{1+ec_0} \\ 0 & c_0 & 0 & 0 & -s_0 & 0 \\ 0 & s_0 & 0 & 0 & c_0 & 0 \end{bmatrix} \tag{13}$$

with $c_0 = \cos\nu_0$ and $s_0 = \sin\nu_0$.

By replacing the true anomaly ν with $w \in \mathbb{R}$ such that:

$$w = \tan(\tfrac{\nu}{2}), \quad \cos\nu = \frac{1-w^2}{1+w^2}, \quad \sin\nu = \frac{2w}{1+w^2} \tag{14}$$

a rational form for equations (11) is obtained:

$$\begin{array}{l} \tilde{x}(w) = \dfrac{p_{x_1}w^4 + p_{x_2}w^3 + p_{x_3}w^2 + p_{x_4}w + p_{x_5}}{(1+w^2)^2} \\ \tilde{y}(w) = \dfrac{p_{y_1}w^2 + p_{y_2}w + p_{y_3}}{1+w^2} \\ \tilde{z}(w) = \dfrac{p_{z_1}w^4 + p_{z_2}w^3 + p_{z_3}w^2 + p_{z_4}w + p_{z_5}}{(1+w^2)^2} \end{array} \tag{15}$$

Denoting $P_x = [p_{x_1}\ p_{x_2}\ p_{x_3}\ p_{x_4}\ p_{x_5}]^T$, $P_y = [p_{y_1}\ p_{y_2}\ p_{y_3}]^T$, $P_z = [p_{z_1}\ p_{z_2}\ p_{z_3}\ p_{z_4}\ p_{z_5}]^T$, it comes:

$$P_x = C_x D \quad P_y = C_y D \quad P_z = C_z D \tag{16}$$

where:

$$C_x = \begin{bmatrix} 0 & 2-e & 1 & 0 & 0 \\ 4-2e & 0 & 0 & 0 & 0 \\ 0 & 2e & 2 & 0 & 0 \\ 4+2e & 0 & 0 & 0 & 0 \\ 0 & -2-e & 1 & 0 & 0 \end{bmatrix} \quad C_y = \begin{bmatrix} 0 & 0 & 0 & -1 & 0 \\ 0 & 0 & 0 & 0 & 2 \\ 0 & 0 & 0 & 1 & 0 \end{bmatrix}$$
$$C_z = \begin{bmatrix} e-1 & 0 & 0 & 0 & 0 \\ 0 & 2-2e & 0 & 0 & 0 \\ -2e & 0 & 0 & 0 & 0 \\ 0 & 2+2e & 0 & 0 & 0 \\ e+1 & 0 & 0 & 0 & 0 \end{bmatrix} \tag{17}$$

A similar approach is used in [12] in order to obtain algebraic expressions for the propagation of the periodic motion, in the case of a periodic motion starting at perigee. The objective of [12] was to determine the type of quadratic surface on which the relative orbit laid. As far as we are concerned, the rational expressions (15) will be used in the purpose of designing maneuvers plans leading to bounded periodic motion after control.

III. Trajectory optimization for autonomous rendezvous

The fixed time impulsive rendezvous problem consists in determining fuel optimal impulsive maneuvers that steer the follower spacecraft from an initial state $X(\nu_1)$ to a desired state $X_f = \begin{bmatrix} x_f & y_f & z_f & \dot{x}_f & \dot{y}_f & \dot{z}_f \end{bmatrix}^T$. An impulsive maneuver involves an ideally instantaneous change ΔV in the spacecraft velocity. The number N of impulsive thrusts is known *a priori* and so are the thrusting instants $\nu_1, ..., \nu_N$. Hence the optimization variables are $\Delta V_1, ..., \Delta V_N \in \mathbb{R}^3$, the coordinates of the thrusts in the local basis of the leader.

A. Proximity periodic relative motion

For our purpose, the terminal condition is relaxed by no longer requiring the follower spacecraft to reach an exact state $X(\nu_N) = X_f$. The objective is to minimize the fuel consumption necessary to reach a final state that can guarantee periodic movement after control, on a trajectory contained in a tolerance region X_{tol}, while taking into account actuators saturation. The optimization problem can be written as:

$$\begin{array}{ll} \min\limits_{\Delta\tilde{V}} & \sum_{i=1}^{N} \|\Delta\tilde{V}_i\|_1 \\ \text{s.t.} & \begin{cases} \|\Delta\tilde{V}_i\| \leq \overline{\Delta\tilde{V}_i},\ \forall\ i = 1...N \\ \tilde{X}(\nu_N) \text{ satisfies (10)} \\ (\tilde{x}(\nu), \tilde{y}(\nu), \tilde{z}(\nu)) \in \tilde{X}_{tol},\ \forall \nu \geq \nu_N \end{cases} \end{array} \tag{18}$$

where $\Delta\tilde{V} = \begin{bmatrix} \Delta\tilde{V}_1 & \cdots & \Delta\tilde{V}_N \end{bmatrix}^T \in \mathbb{R}^{3N}$ and $\overline{\Delta\tilde{V}_i} \in \mathbb{R}^3$ are the thrusters saturation levels. $\tilde{X}(\nu_N)$ is the state at the end of control, which considering (8) can be expressed as:

$$\tilde{X}(\nu_N) = A_N + B_N\Delta\tilde{V} \tag{19}$$

with:

$$A_N = \Phi_{\nu_1}^{\nu_N}\tilde{X}(\nu_1) \quad B_N = \begin{bmatrix} \Phi_{\nu_1}^{\nu_N}\tilde{B} \cdots \Phi_{\nu_{N-1}}^{\nu_N}\tilde{B}\ \tilde{B} \end{bmatrix}. \tag{20}$$

Since the 1-norm criterion is only piecewise linear, slack variables $Z \in \mathbb{R}^{3N}$ are introduced in order to write J in a linear form. Z are such that:

$$\begin{cases} -Z_i \leq \Delta\tilde{V}_i \leq Z_i \\ Z_i \leq \overline{\Delta\tilde{V}_i} \end{cases} , \ \forall\ i = 1, \cdots, N \tag{21}$$

Let $M(\nu_N)$ be:

$$M(\nu_N) = \begin{bmatrix} 0 & 0 & -\frac{2+3e\cos\nu_N+e^2}{(1+e\cos\nu_N)^2} & 1 & 0 & -\frac{e\sin\nu_N}{1+e\cos\nu_N} \end{bmatrix} \tag{22}$$

Then the periodicity constraint (10) can be written as:

$$M(\nu_N)\tilde{X}(\nu_N) = 0 \tag{23}$$

The tolerance region X_{tol} is a box centered on the final position X_f, defined by $X_{tol} = \begin{bmatrix} x_{tol} & y_{tol} & z_{tol} \end{bmatrix}$. The variable change (4) must be taken into consideration when writing the tolerance box constraints on the autonomously propagated trajectory:

$$\begin{array}{l} (1+e\cos\nu)(x_f - x_{tol}) \leq \tilde{x}(\nu) \leq (1+e\cos\nu)(x_f - x_{tol}) \\ (1+e\cos\nu)(y_f - y_{tol}) \leq \tilde{y}(\nu) \leq (1+e\cos\nu)(y_f - y_{tol}) \\ (1+e\cos\nu)(z_f - z_{tol}) \leq \tilde{z}(\nu) \leq (1+e\cos\nu)(z_f - z_{tol}) \end{array} \tag{24}$$

Constraints (24) must be respected for all instants starting from the end of the plan ($\forall \nu \geq \nu_N$). The optimization problem (18) becomes:

$$\min_{Z,\Delta\tilde{V}} \quad \sum_{i=1}^{N} Z_i$$
$$\text{s.t.} \quad \begin{cases} -Z_i \leq \Delta\tilde{V}_i \leq Z_i \\ Z_i \leq \overline{\Delta\tilde{V}_i} \end{cases}, \ \forall\ i = 1...N$$
$$M(\nu_N)\tilde{X}(\nu_N) = 0$$
$$\begin{cases} \tilde{x}_f - \tilde{x}_{tol} \leq \tilde{x}(\nu) \leq \tilde{x}_f + \tilde{x}_{tol} \\ \tilde{y}_f - \tilde{y}_{tol} \leq \tilde{y}(\nu) \leq \tilde{y}_f + \tilde{y}_{tol} \\ \tilde{z}_f - \tilde{z}_{tol} \leq \tilde{z}(\nu) \leq \tilde{z}_f + \tilde{z}_{tol} \end{cases}, \ \forall \nu \geq \nu_N \tag{25}$$

The LP approach for solving (25) presented in [8] requires the discretization of constraints (24) over a specified interval $[\nu_{N+1}, \nu_{N+q}]$ after control:

$$\begin{array}{l} \tilde{x}_f - \tilde{x}_{tol} \leq \tilde{x}(\nu_k) \leq \tilde{x}_f + \tilde{x}_{tol} \\ \tilde{y}_f - \tilde{y}_{tol} \leq \tilde{y}(\nu_k) \leq \tilde{y}_f + \tilde{y}_{tol} \\ \tilde{z}_f - \tilde{z}_{tol} \leq \tilde{z}(\nu_k) \leq \tilde{z}_f + \tilde{z}_{tol} \end{array}, \forall\ k \in \{N+1, ..., N+q\} \tag{26}$$

with q the number of discrete points where constraints are explicitly checked. This approach cannot guarantee that the box constraints (24) are not violated between the discretization points.

The variable change (14) can be used to define rational bounds for each coordinate. Please note that the methodology is detailed only for the x axis. The y and z axis follow the same procedure.

$$\begin{array}{l} \tilde{x}_{\max}(w) = \frac{(1-e)w^2+1+e}{1+w^2}(x_f + x_{tol}) \\ \tilde{x}_{\min}(w) = \frac{(1-e)w^2+1+e}{1+w^2}(x_f - x_{tol}) \end{array} \tag{27}$$

Using equations (15) and (27), the tolerance box constraints (24) can be written as rational inequalities:

$$\tilde{x}_{\min}(w) \leq \tilde{x}(w) \leq \tilde{x}_{\max}(w), \quad \forall w \in \mathbb{R} \tag{28}$$

Let $\overline{x}$ and $\underline{x}$ be:

$$\begin{array}{l} \overline{x}(w) = -\tilde{x}(w) + \tilde{x}_{\max}(w) = \frac{1}{(1+w^2)^2}\Gamma_{\overline{x}}(w) \\ \underline{x}(w) = \tilde{x}(w) - \tilde{x}_{\min}(w) = \frac{1}{(1+w^2)^2}\Gamma_{\underline{x}}(w) \end{array} \tag{29}$$

where $\Gamma_{\overline{x}}$ and $\Gamma_{\underline{x}}$ are the following polynomials:

$$\Gamma_{\overline{x}}(w) = \sum_{i=1}^{5} \gamma_{\overline{x}_i} w^{i-1} \quad \Gamma_{\underline{x}}(w) = \sum_{i=1}^{5} \gamma_{\underline{x}_i} w^{i-1} \tag{30}$$

whose coefficients $\gamma_{\overline{x}} = \begin{bmatrix} \gamma_{\overline{x}_1} & \gamma_{\overline{x}_2} & \gamma_{\overline{x}_3} & \gamma_{\overline{x}_4} & \gamma_{\overline{x}_5} \end{bmatrix}^T$ and $\gamma_{\underline{x}} = \begin{bmatrix} \gamma_{\underline{x}_1} & \gamma_{\underline{x}_2} & \gamma_{\underline{x}_3} & \gamma_{\underline{x}_4} & \gamma_{\underline{x}_5} \end{bmatrix}^T$ are given by:

$$\begin{array}{l} \gamma_{\overline{x}} = -P_x + T(x_f + x_{tol}) \\ \gamma_{\underline{x}} = P_x - T(x_f - x_{tol}) \end{array} \tag{31}$$

and $T = \begin{bmatrix} 1-e & 0 & 2 & 0 & 1+e \end{bmatrix}^T$. Using (12), (16) and (19) it comes:

$$\begin{array}{l} \gamma_{\overline{x}} = -C_x C(\nu_N) B_N \Delta\tilde{V} - C_x C(\nu_N) A_N + T(x_f + x_{tol}) \\ \gamma_{\underline{x}} = C_x C(\nu_N) B_N \Delta\tilde{V} + C_x C(\nu_N) A_N - T(x_f - x_{tol}) \end{array} \tag{32}$$

Hence the coefficients $\gamma_{\overline{x}}$ and $\gamma_{\underline{x}}$ of the polynomials $\Gamma_{\overline{x}}$ and $\Gamma_{\underline{x}}$ depend linearly on the optimization variables $\Delta\tilde{V}$.

The box constraints (28) can be expressed as non-negativity conditions on $\overline{x}$ and $\underline{x}$. However, since the denominator $(1+w^2)^2$ is always strictly positive, these conditions are equivalent to the non-negativity of the polynomials $\Gamma_{\overline{x}}$ and $\Gamma_{\underline{x}}$:

$$\begin{array}{l} \Gamma_{\overline{x}}(w) \geq 0 \\ \Gamma_{\underline{x}}(w) \geq 0 \end{array}, \forall w \in \mathbb{R}. \tag{33}$$

As showed in [13], the cone of non-negative univariate polynomials can be seen as the linear image of the cone of positive semi-definite matrices. Thus, finding non-negative polynomials over an infinite interval becomes a semi-definite programming problem.

Let P be a polynomial of degree $2n$. Searching for $p_i,\ i = 1..2n+1$, the coefficients of the polynomial P, such that $P(w) = \sum_{i=1}^{2n+1} p_i w^{i-1} \geq 0,\ \forall\ w \in \mathbb{R}$ is equivalent to searching for a symmetrical positive semi-definite matrix $Y \in \mathbb{R}^{(n+1)\times(n+1)} \succeq 0$, such that [13]:

$$p_i = \text{tr}(Y H_{n,i}),\ i = 1..2n+1 \tag{34}$$

where $H_{n,i} \in \mathbb{R}^{(n+1)\times(n+1)}$ are the Henkel matrices:

$$H_{n,i}(j,k) = \begin{cases} 1, \text{ if } j+k = i+1 \\ 0, \text{otherwise} \end{cases} \tag{35}$$

and *tr* denotes the trace of the matrix.

The same principle is applied for the polynomial constraints (33). If there exist two symmetric positive semi-definite matrices $Y_{\overline{x}} \in \mathbb{R}^{(n+1)\times(n+1)} \succeq 0$ and $Y_{\underline{x}} \in \mathbb{R}^{(n+1)\times(n+1)} \succeq 0$ such that the coefficients of the polynomials $\Gamma_{\overline{x}}$ and $\Gamma_{\underline{x}}$ are equal to:

$$\begin{array}{l} \gamma_{\overline{x}} = \begin{bmatrix} \text{tr}(Y_{\overline{x}} H_{n,1}) & \dots & \text{tr}(Y_{\overline{x}} H_{n,2n+1}) \end{bmatrix}^T \\ \gamma_{\underline{x}} = \begin{bmatrix} \text{tr}(Y_{\underline{x}} H_{n,1}) & \dots & \text{tr}(Y_{\underline{x}} H_{n,2n+1}) \end{bmatrix}^T \end{array} \tag{36}$$

then constraints (33) are guaranteed to be satisfied *continuously* ($\forall w \in \mathbb{R}$).

The optimization problem (25) becomes a semi-definite program (SDP):

$$\min_{Z,\Delta\tilde{V}} \quad \sum_{i=1}^{N} Z_i$$
$$\text{s.t.} \quad \begin{cases} -Z_i \leq \Delta\tilde{V}_i \leq Z_i \\ Z_i \leq \overline{\Delta\tilde{V}_i} \end{cases}, \ \forall\ i = 1 \dots N$$
$$M(\nu_N)\tilde{X}(\nu_N) = 0$$
$$Y_{\overline{x}} \succeq 0 \quad Y_{\overline{y}} \succeq 0 \quad Y_{\overline{z}} \succeq 0$$
$$Y_{\underline{x}} \succeq 0 \quad Y_{\underline{y}} \succeq 0 \quad Y_{\underline{z}} \succeq 0$$
$$\begin{array}{l} \gamma_{\overline{x}} = [\text{tr}(Y_{\overline{x}} H_{2,1}) \dots \text{tr}(Y_{\overline{x}} H_{2,5})]^T \\ \gamma_{\underline{x}} = [\text{tr}(Y_{\underline{x}} H_{2,1}) \dots \text{tr}(Y_{\underline{x}} H_{2,5})]^T \\ \gamma_{\overline{y}} = [\text{tr}(Y_{\overline{y}} H_{1,1}) \dots \text{tr}(Y_{\overline{y}} H_{1,3})]^T \\ \gamma_{\underline{y}} = [\text{tr}(Y_{\underline{y}} H_{1,1}) \dots \text{tr}(Y_{\underline{y}} H_{1,3})]^T \\ \gamma_{\overline{z}} = [\text{tr}(Y_{\overline{z}} H_{2,1}) \dots \text{tr}(Y_{\overline{z}} H_{2,5})]^T \\ \gamma_{\underline{z}} = [\text{tr}(Y_{\underline{z}} H_{2,1}) \dots \text{tr}(Y_{\underline{z}} H_{2,5})]^T \end{array} \tag{37}$$

B. Always feasible formulation

When solving an optimization problem like problem (37) as part of an autonomous rendezvous algorithm, it is important to guarantee *at each step* the feasibility of the solution. Infeasibility could arise from the fact that the objective cannot be reached in the N steps of the plan (because the control action is bounded by saturation constraints) or from the fact that no periodic trajectory could be found in the given tolerance region.

Infeasibility can be avoided by considering the dimensions of the tolerance box as optimization parameters. For the LP formulation of the problem, feasibility is guaranteed by using a scale factor for the tolerance box [9]. In our case, each dimension of the tolerance box is considered as a separate parameter. As illustrated by equations (32), the coefficients of the polynomials that constitute the constraints depend linearly on X_{tol}. So transforming X_{tol} into a decision variable does not change the nature of the optimization problem and does not increase its complexity.

The optimization criterion must be modified to include the new variables:

$$\min_{Z,\Delta\bar{V},X_{tol}} \quad \sum_{i=1}^{N} Z_i + \rho \sum_{i=1}^{3} X_{tol}(i) \tag{38}$$

where $\rho > 0$ is large enough to ensure that the tolerance box is modified only when needed to guarantee feasibility.

Bounds should be given for the minimal box X_m, to ensure that the optimization algorithm will not minimize the box and as a consequence increase the fuel consumption:

$$X_{tol} \geq X_m \tag{39}$$

IV. Numerical Examples

To illustrate our approach for finding the optimal solution to (18), we used a Prisma rendezvous mission, whose scenario information is given in Table. I. The problem was solved in Matlab using Yalmip [14] and SeDuMi [15]. For comparison, we used the solution obtained from the LP approach, as presented in [8]. The LP problem was resolved with the Matlab's linear solver *linprog*, using 15 discretization points over 1 period for the tolerance box constraints.

The maneuvers plans obtained with each method yielded very close values for the optimization criterion. But the advantage of our methodology can be noticed when looking at the trajectories obtained after control, in Fig. 2. For the LP formulation, the box constraints are violated between some of the discretization instants. Our methodology produced trajectories that evolve very close to the bounds, without crossing them. It guarantees continuous satisfaction of the constraints, without adding extra inequalities to reach a certain precision.

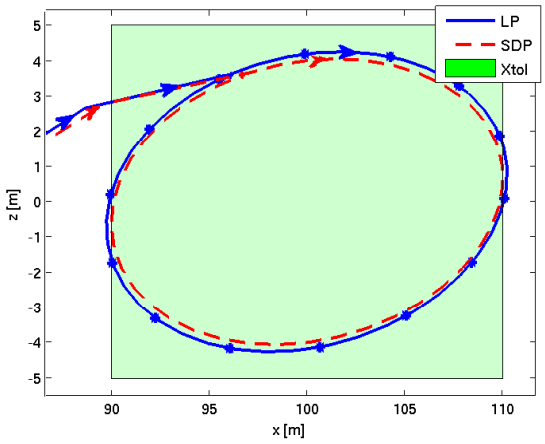

Fig. 2. xz axis projections of the periodic relative trajectory after control

For better understanding, Table II shows the influence on the performances of the LP based algorithm of the number of instants where constraints are explicitly checked. The same simulation data as for the first example is used. The discretization is done over 1 orbital period ($T = 5843$s), taking 15, 30 and then 50 instants. The given solver time (ST) is the mean time for 10 runs of each algorithm. The cost is the sum of ΔV (passing back to the original variables).

The costs obtained with each method are very similar. It can be easily observed that for the LP based algorithms increasing the number of discretization points increases the solver time and the number of constraints. On the other hand, it decreases the time spent outside the box (TOB), where the tolerance box constraints on the trajectory are violated. However, a large number of points would be necessary to get closer to the performances of the SDP approach (zero violation of the constraints).

A slightly different Prisma mission is used to illustrate the advantages of the always feasible formulation. The changes to the rendezvous scenario are given in Table III.

In the always feasible case, the obtained solution suggests

TABLE I
SIMULATION DATA

Eccentricity (e)	0.023776
Semi-major axis (a) [m]	7 011 003
Transfer time [s]	64620
Initial time [s]	1282
Actuator saturation ($\Delta\bar{v}$) [m/s]	0.26
Impulsive thrusts (N)	10
Initial state [m,m/s]	[10000,0,0,0,0,0]
Final state (X_f) [m,m/s]	[100,0,0,0,0,0]
Position tolerance (X_{tol}) [m]	[10,5,5]

TABLE II
ALGORITHMS COMPARISON

Method	Cost [m/s]	ST [s]	TOB[s]	Constraints	Variables
LP15	0.390962	1.0969	818	271	60
LP30	0.390983	2.0195	234	451	60
LP50	0.390985	1.4937	152	691	60
SDP	0.390986	0.9387	0	133	90

TABLE III

SIMULATION DATA

Transfer time [s]	18000
Final state X_f [m,m/s]	[300,0,30,0,0,0]
Minimum box X_m [m]	[1,1,1]

that a box larger than X_m is needed to ensure feasibility. As shown in Fig. 3, $X_{tol} = [1, 1, 33.0664]$ so an expansion on the z axis of the given tolerance region is necessary.

Used in an open-loop scheme, the always feasible formulation can provide some insight to the size of the smallest tolerance box that ensures feasibility. Integrated in a closed-loop scheme, it can help avoiding unwanted situations where no solution is available.

V. CONCLUSIONS

In this paper a new method for obtaining an open-loop impulsive maneuvers plan leading to periodic proximity relative motion, between two spacecraft on Keplerian orbits was presented. The periodic relative trajectory is confined inside a specified tolerance region. By using the rational expressions for the propagation of the periodic motion and the result linking the cone of non-negative polynomials to the cone of semi-definite positive matrices, the requirement to define a prediction horizon where constraints are explicitly checked for a finite number of instants was removed. The method guarantees constraints satisfaction all along the path, without increasing the computational load or the fuel consumption. An always feasible formulation of the problem was also given, by considering the dimensions of the tolerance region as optimization parameters.

REFERENCES

[1] D. J. J. Irvin, R. Cobb, and T. Lovell, "Fuel-Optimal Maneuvers for Constrained Relative Satellite Orbits," *Journal of guidance, control, and dynamics*, vol. 32, no. 3, pp. 960–973, 2009.

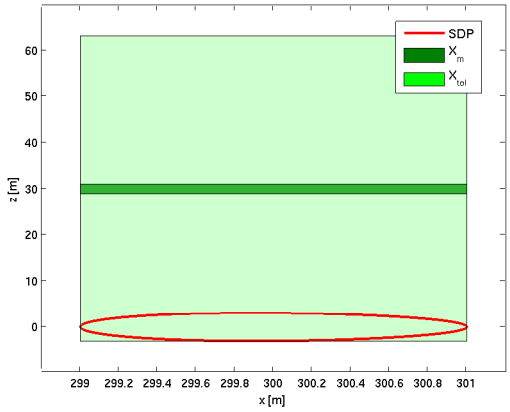

Fig. 3. *xz* axis projections of the periodic relative trajectory after control; the clear green rectangle defines the new tolerance region

[2] P. Gurfil, "Relative Motion between Elliptic Orbits: Generalized Boundedness Conditions and Optimal Formationkeeping," *Journal of Guidance, Control, and Dynamics*, vol. 28, no. 4, pp. 761–767, July 2005.

[3] T. Alfriend and H. Schaub, "Dynamics and Control of Spacecraft Formations: Challenges and Some Solutions," *Journal of the Astronautical Sciences*, vol. 48, no. 2, pp. 249–267, 2000.

[4] G. Inalhan, J. P. How, and M. Tillerson, "Relative Dynamics and Control of Spacecraft Formations in Eccentric Orbits," *Journal of Guidance, Control, and Dynamics*, vol. 25, no. 1, pp. 48–59, Jan. 2002.

[5] P. Sengupta and S. R. Vadali, "Relative Motion and the Geometry of Formations in Keplerian Elliptic Orbits," *Journal of Guidance, Control, and Dynamics*, vol. 30, no. 4, pp. 953–964, 2007.

[6] P. Gurfil and K. Kholshevnikov, "Manifolds and Metrics in the Relative Spacecraft Motion Problem," *Journal of Guidance, Control, and Dynamics*, vol. 29, no. 4, pp. 1004–1010, July 2006.

[7] K. Kholshevnikov and N. Vassiliev, "Natural Metrics in the Spaces of Elliptic Orbits," *Celestial Mechanics and Dynamical Astronomy*, vol. 89, no. 2, pp. 119–125, 2004.

[8] L. S. Breger, G. Inalhan, M. Tillerson, and J. P. How, "Cooperative Spacecraft Formation Flying: Model Predictive Control with Open- and Closed-Loop Robustness," in *Modern Astrodynamics*, P. Gurfil, Ed. Butterworth-Heinemann, 2007, ch. 8, pp. 237–277.

[9] M. Tillerson, G. Inalhan, and J. P. How, "Co-ordination and control of distributed spacecraft systems using convex optimization techniques," *International Journal of Robust and Nonlinear Control*, vol. 12, no. 2-3, pp. 207–242, Feb. 2002.

[10] J. Tschauner, "Elliptic orbit rendezvous," *AIAA Journal*, vol. 5, no. 6, pp. 1110–1113, 1967.

[11] K. Yamanaka and F. Ankersen, "New state transition matrix for relative motion on an arbitrary elliptical orbit," *Journal of guidance, control, and dynamics*, vol. 25, no. 1, pp. 60–66, 2002.

[12] F. Jiang, J. Li, H. Baoyin, and Y. Gao, "Study on Relative Orbit Geometry of Spacecraft Formations in Elliptical Reference Orbits," *Journal of Guidance, Control, and Dynamics*, vol. 31, no. 1, pp. 123–134, 2008.

[13] Y. Nesterov, "Squared functional systems and optimization problems," in *High Performance Optimization*. Kluwer Academic Publishers, 2000, ch. 17, pp. 405–440.

[14] J. Lofberg, "YALMIP : a toolbox for modeling and optimization in MATLAB," in *2004 IEEE International Conference on Robotics and Automation*. Ieee, 2004, pp. 284–289.

[15] J. Sturm, "Using SeDuMi 1.02, A Matlab toolbox for optimization over symmetric cones," *Optimization Methods and Software*, vol. 11, no. 1, pp. 625–653, 1999.